THE EFFECTS OF BORON ADDITION AND PRESULFIDATION TEMPERATURE ON THE HDS ACTIVITY OF A Co-MoS_2/Al_2O_3 CATALYST

Usman, Takeshi Kubota, and Yasuaki Okamoto*

Department of Material Science, Shimane University
Matsue, 690-8504, Japan

Received 29 April 2005; Accepted 30 May 2005

ABSTRACT

The effect of boron addition was studied on the hydrodesulfurization (HDS) of thiophene over Co-$MoS_2/B/Al_2O_3$ (CVD-Co/$MoS_2/B/Al_2O_3$), which was prepared by a CVD technique using $Co(CO)_3NO$ as a precursor of Co. The catalyst was characterized by means of NO adsorption, XPS, Raman Spectroscopy, FTIR, and TEM. The HDS activity of CVD-Co/$MoS_2/B/Al_2O_3$ catalyst increased as the boron content increased up to about 0.6 and 1.2 wt% B for the catalyst presulfided at 673 and 773 K respectively, followed by a decrease with a further addition of boron loading. In spite of the activity increase, the amount of NO adsorption on $MoS_2/B/Al_2O_3$ steadily decreased with increasing boron loading, suggesting that the dispersion of MoS_2 particles is decreased by the addition of boron. Selective formation of the CoMoS phase on CVD-Co/$MoS_2/B/Al_2O_3$ was achieved by the CVD technique. The TOF of the HDS over the CVD-Co/$MoS_2/B/Al_2O_3$ catalyst, defined by the activity per Co atom forming the CoMoS phase, increased as high as 1.6 and 1.9 times for the catalyst presulfided at 673 and 773 K, respectively. It is concluded that the addition of boron weakens the interaction between Mo oxides and Al_2O_3 surface, promoting the formation of the so called Co-Mo-S "pseudo" type II over CVD-Co/$MoS_2/B/Al_2O_3$ presulfided at 673 K. The Co-Mo-S "pseudo" type II is a metastable phase with the TOF value intermediate between Co-Mo-S type I and type II. With CVD-Co/$MoS_2/B/Al_2O_3$ presulfided at 773 K, the addition of boron promotes the formation of "real" Co-Mo-S type II, possibly by the formation of well-crystallized MoS_2 structure.

Keywords: *Hydrodesulfurization; Co-Mo sulfide catalysts; Effect of boron addition; CVD technique; Turnover frequency*

INTRODUCTION

Regulation about decreasing the sulfur content in petroleum feedstocks has become more and more strict in order to protect the environment and the living things. Hydrodesulfurization (HDS) of petroleum feedstocks has been, therefore, an indispensable reaction to produce clean fuels [1]. Sulfided Mo or W-based catalysts promoted by nickel and/or cobalt have been widely used for industrial HDS reaction [2,3]. Numerous studies [2-5] have already been devoted to understand the structure and reactivity of the catalytically active sites, the microscopic reaction mechanisms of HDS and hydrogenation, the effect of support and additives and so on. In spite of the fact that the HDS catalysts have been improved considerably, the catalytic performance is still required to be improved more to meet more severe requirements of legislative restriction of sulfur content in petroleum products [6].

Addition of boron has been reported to modify the dispersion of Mo on the surface of alumina [7,8]. The effect of boron addition on the activity of Co-Mo or Ni-Mo/Al_2O_3 catalysts has been widely studied [7,9-11]. Although some workers reported that the high acidity of alumina boria system increased the hydrocracking [9] and HDN [9-11] activity of Ni-Mo/B/Al_2O_3, many conflicting results were obtained in the previous studies. Li *et al.* [9] believed that the addition of boron up to 1 mol% increased the activity of Ni-Mo/Al_2O_3 catalysts for HDS of DBT, in contrast to the results by Lewandowski and Sarbak [10] that boron addition did not affect the activity of Ni-Mo/Al_2O_3 catalysts for the HDS of coal liquid. Stranick *et al.* [12] believed that the addition of boron to Al_2O_3 can improve the dispersion of Co and change the chemical states of Co in Co/Al_2O_3 catalysts. In addition, Morishige and Akai [8] indicated that boron addition decreased the dispersion of Mo in Mo/Al_2O_3 catalyst and weakens the interactions between Mo species and the Al_2O_3 surface. Thus, it is expected that boron added to Co-Mo or Ni-Mo/Al_2O_3 modifies both Mo and Co(Ni) species. It will be easy to understand the effects of boron addition if we could separate the effects of

* Corresponding author.
Email address : yokamoto@riko.shimane-u.ac.jp

boron addition on Mo and Co phases. In the present study, we tried to clarify the effect of boron addition on the Co-Mo-S phase supported on Al_2O_3.

In a previous study [13-16], we have shown that when a supported Mo sulfide catalyst is exposed to a vapor of $Co(CO)_3NO$ (CVD-technique), followed by evacuation and resulfidation, the Co species in the resultant CVD-Co/MoS_2 catalysts are selectively transformed into the Co-Mo-S phase and accordingly the amount of Co in the catalyst represents the amount of the Co-Mo-S phase. In the CVD-Co/MoS_2 catalysts, the edge of MoS_2 particles is fully covered by the Co-Mo-S phase. It is, therefore, expected that the CVD-technique provides a strong clue to understand the nature of the boron addition to Co/MoS_2/Al_2O_3 catalysts. In the present study, we investigated the effect of boron addition on the HDS activity of CVD-Co/MoS_2/Al_2O_3 catalysts to understand the effects in terms of the number of active sites and their intrinsic activity.

EXPERIMENTAL SECTION

Catalyst Preparation

A series of Mo/Al_2O_3-B_2O_3 was prepared by a double impregnation technique. γ-Al_2O_3 (180 m^2 g^{-1}) was first impregnated with a H_3BO_3 solution, followed by a calcination at 773 K for 5 h. The boron contents were 0.3, 0.6, 0.9, 1.2, and 2.5 wt% B. Then, the Al_2O_3-B_2O_3 materials were impregnated with $(NH_4)_6Mo_7O_{24}.4H_2O$ and calcined at 773 K for 5 h. The Mo loading was 13 wt% MoO_3. The catalyst was presulfided at either 673 K for 1.5 h or 773 K for 2 h in a stream of H_2S/H_2. The detailed procedures have been described elsewhere [7,13].

Co-Mo/B/Al_2O_3 catalysts were prepared by introducing $Co(CO)_3NO$ into MoS_2/B/Al_2O_3 by means of a chemical vapor deposition (CVD) technique. The CVD technique has been described in detail previously [13,14]. In brief, a vapor pressure of $Co(CO)_3NO$ at 273 K was used to prepare $Co(CO)_3NO$/MoS_2/B/Al_2O_3, followed by a sulfidation at 673 K in a 10% H_2S/H_2 stream. The catalyst thus prepared is denoted CVD-Co/MoS_2/B/Al_2O_3 followed by the presulfidation temperature in parentheses if necessary, hereinafter. The amount of Co was analyzed by XRF. The detailed procedures have been described elsewhere [16].

Reaction Procedure

The initial activity of the freshly prepared catalyst for the HDS of thiophene was evaluated at 623 K using a circulation reaction system made of glass under mild reaction conditions (initial H_2 pressure, 20 kPa). The HDS activity was calculated on the basis of the accumulated amount of H_2S. The detailed reaction procedures have been reported previously [13].

Characterization

The amount of NO adsorption on a catalyst was measured at room temperature by a pulse technique after cooling the catalyst sample from the presulfidation temperature in a 10% H_2S/H_2 stream. The sample was purged for 15 min with a He stream before periodical admissions of a pulse of 10% NO/He. The detailed procedures have been reported elsewhere [13,17].

The FTIR spectra of B/Al_2O_3 were recorded in a transmission mode at room temperature on a single-beam FTIR spectrophotometer (JASCO, FTIR-620V). A self-supporting wafer of B/Al_2O_3 (32 mg cm^{-2}) was evacuated in an *in situ* IR cell at 773 K for 1 h (< 1 x 10^{-3} Pa). After the sample was cooled to room temperature, IR spectra were measured and the background spectrum was subtracted. The spectra of calcined-Al_2O_3 (ALO-7) and MoO_3/B/Al_2O_3 (2.5 wt% B) were also recorded for comparison.

The Laser Raman spectra of MoO_3/B/Al_2O_3 were obtained at room temperature in air on an NRS-2100 spectrometer (JASCO) equipped with a CCD detector. The 514.5 nm line of an Ar^+ laser was used for excitation at an intensity of 10 mW at the source.

The XP spectra of MoO_3/B/Al_2O_3 catalyst samples were measured on an ESCA 750 spectrometer (Shimadzu) using a Mg $K\alpha_{1,2}$ radiation (1253.6 eV). The sample powder was mounted on a holder using a double adhesive tape. The binding energies were referenced to the Al2p level (74.5 eV) due to Al_2O_3.

TEM observations were made on an electron microscope Hitachi H-800 with an accelerating voltage of 200 keV for CVD-Co/MoS2/B/Al2O3 (673). The catalyst sample was dispersed in heptane in an N_2-filled glove-bag. The distributions of MoS_2 or WS_2 slab size and stacking number were calculated over 350-450 particles.

RESULTS AND DISCUSSION

Fig. 1 depicts the thiophene HDS activity over CVD-Co/MoS_2/B/Al_2O_3 catalyst as a function of B content. It is clearly shown in Fig. 1, the addition of a proper amount of boron increased the HDS activity of CVD-Co/MoS_2/B/Al_2O_3 catalyst, irrespective of the presulfidation temperature. The optimum loading of boron was ca. 0.6 and 1.2 wt%

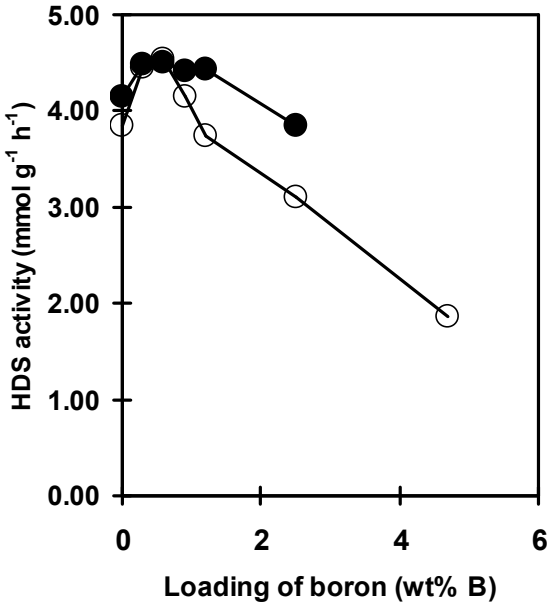

Figure 1 HDS activity of CVD-Co/MoS_2/B/Al_2O_3 presulfided at 673 K (open symbol) and 773 K (closed symbol) as a function of boron loading

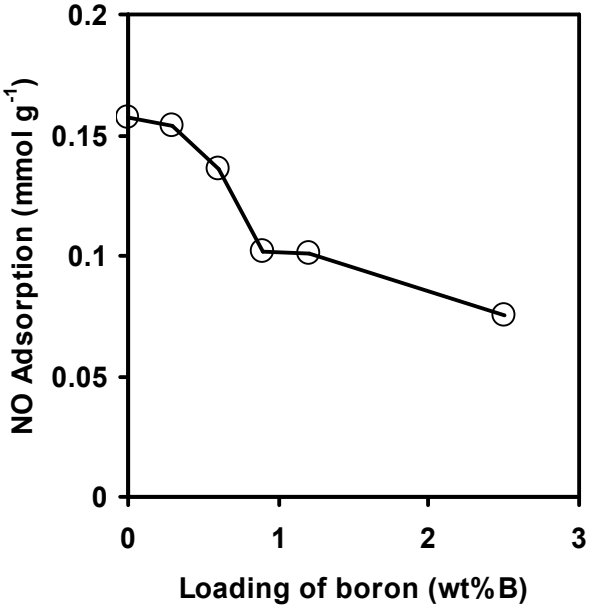

Figure 2 NO adsorption of MoS_2/B/Al_2O_3 pre-sulfided at 673 K as a function of boron loading.

B for CVD-Co/MoS_2/B/Al_2O_3 (673) and CVD-Co/MoS_2/B/Al_2O_3 (773), respectively. The HDS activity decrease at a higher boron loading was more prominent for CVD-Co/MoS_2/B/Al_2O_3 (673) compared to that of CVD-Co/MoS_2/B/Al_2O_3 (773). In conformity with the present results, Ramírez *et al.* [18] reported that boron addition into Co-Mo/Al_2O_3 catalysts enhanced thiophene HDS activity and the maximum activity was attained at the boron content of 0.8 wt% B.

In spite of the activity increases in Fig. 1, the amount of NO adsorption on MoS_2/B/Al_2O_3 decreased with increasing B loading as shown in Fig. 2. Taking into consideration the selective adsorption of NO molecules on the edge sites of MoS_2 particles [19], the results in Fig. 2 suggest that the dispersion of MoS_2 clusters is decreased by the addition of boron.

The amount of Co anchored by the CVD technique over MoS_2/B/Al_2O_3 is summarized in Table 1. Obviously, it decreased as the boron content increased. Fig. 3 shows the Co/Mo atomic ratio of the CVD-Co/MoS_2/B/Al_2O_3 catalysts as a function of the NO/Mo ratio of the MoS_2/B/Al_2O_3 samples. The Co/Mo ratio is proportional to the NO/Mo ratio, this being in conformity with our previous results for CVD-Co/MoS_2/support (support: Al_2O_3, TiO_2, ZrO_2, and SiO_2) [13]. Taking into consideration selective adsorption of NO molecules on the edges of MoS_2 particles, the proportional correlation in Fig. 3 demonstrates that the Co sulfide species admitted by the CVD technique are located on the edges of MoS_2 particles in MoS_2/B/Al_2O_3.

Table 1 Amount of cobalt content and TOF over CVD-Co/MoS_2/B/Al_2O_3 catalysts

Boron content (wt% B)	Cobalt loading (wt%)	TOF (h^{-1})	
		Presulfided at 673 K	Presulfided at 773 K
0	2.70	8.4	8.35
0.3	2.45	10.7	10.43
0.6	2.33	11.5	11.65
0.9	1.81	13.5	13.9
1.2	1.67	13.3	16.2
2.5	1.54	12	16
4.7	0.84	13.1	--

In order to explain the activity increase of CVD-Co/MoS_2/B/Al_2O_3 in Fig. 1, the TOF (turnover frequency, h^{-1}) of the reaction is plotted in Fig. 4 against the loading of boron. We calculated the TOF on the basis of the Co content in the catalyst. It is clearly shown from Fig. 4 that the TOF is increased by the addition of boron up to ca. 0.8 and 1.2 wt% B for CVD-Co/MoS_2/B/Al_2O_3 (673) and CVD-Co/MoS_2/B/Al_2O_3 (773), respectively, and this trend levels off with a further addition of boron. Topsøe *et al.* [2], defined two types of the Co-Mo-S phase depending on the intrinsic activity, Co-Mo-S type I and type II. Co-Mo-S type II, which is formed by high temperature sulfidation (875-1275 K), is about two times more active for the HDS of thiophene than Co-Mo-S type I formed by low temperature sulfidation (675 K). Based on the definition by Topsøe, the TOF over boron-free CVD-Co/MoS_2/Al_2O_3 presulfided at 673 K is concluded as Co-Mo-S type I

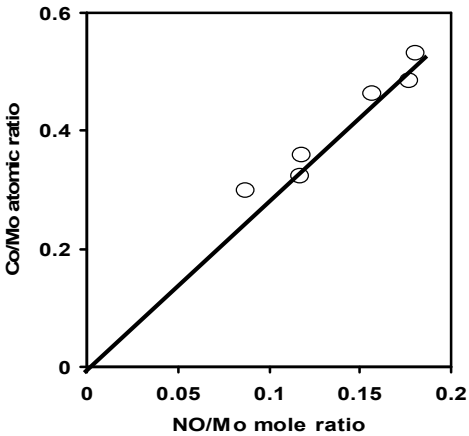

Figure 3 Correlation between the Co/Mo atomic ratio and NO/Mo mole ratio as a function of boron loading. The catalyst presulfided at 673 K.

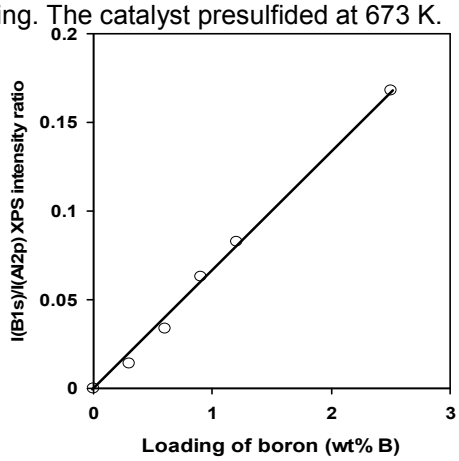

Figure 5 I(B1s)/I(Al2p) XPS intensity ratio for $MoO_3/B/Al_2O_3$ as a function of boron loading. A theoretical line assuming a monolayer dispersion of B is shown.

The TOF over CVD-Co/MoS_2/B/Al_2O_3 (673) (> 0.8 wt% B) is 1.6 times as high as that of boron-free CVD-Co/MoS_2/Al_2O_3 (673), being in agreement with the previous study on CVD-Co/MoS_2/SiO_2 [13]. On the basis of the results, we previously concluded the formation of Co-Mo-S type II in CVD-Co/MoS_2/B/Al_2O_3 (673) [7] as well as CVD-Co/MoS_2/SiO_2 (673) [13]. However, as shown in Fig.5, the TOF over CVD-Co/MoS_2/B/Al_2O_3 is further increased by the presulfidation at 773 K. The TOF over CVD-Co/MoS_2/B/Al_2O_3 (773) is 1.9 times as high as that over boron-free CVD-Co/MoS_2/Al_2O_3 (673). The extent of the increase in TOF being consistent with that reported by Topsøe *et al.* [2] for the shift from Co-Mo-S type I to type II. Accordingly, it is concluded that the Co-Mo-S phase in CVD-Co/MoS_2/B/Al_2O_3 (773) is classified to "real" Co-Mo-S type II defined by Topsøe *et al.* [2]. The Co-Mo-S phase, which is observed for CVD-Co/MoS_2/B/Al_2O_3 (673), with a TOF value intermediate between Co-Mo-S type II and type I, is defined as Co-Mo-S "pseudo" type II hereinafter.

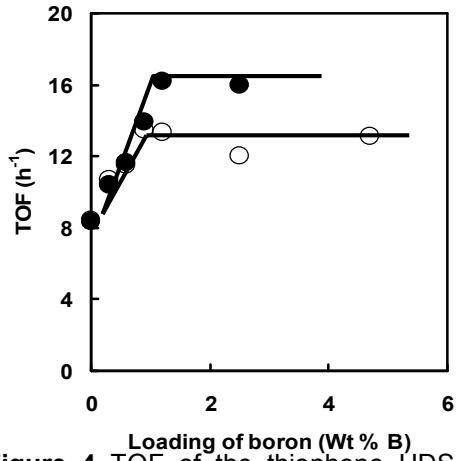

Figure 4 TOF of the thiophene HDS over CVD-Co/MoS_2/B/Al_2O_3 presulfided at 673 K (open circle) and 773 K (closed circle) as a function of boron loading.

On the basis of the results, we instead propose that Co-Mo-S pseudo type II and type II are formed on the edge of fully sulfided MoS_2 particles having no strong interactions with the support in contrast to Co-Mo-S type I and that pseudo type II is correlated to a distorted structure of MoS_2 particles, while type II to a well crystallized MoS_2 structure. We concluded that there are, at least, two roles of boron addition to CVD-Co/MoS_2/Al_2O_3 that is boron weakens the interaction between Mo oxides and Al_2O_3 surface, promoting the formation of CoMoS pseudo type II over CVD-Co/MoS_2/B/Al_2O_3 (673), and boron accelerates the formation of well crystallized MoS_2 structure to form the "real" CoMoS type II over CVD-Co/MoS_2/B/Al_2O_3 (773).

In order to evaluate the dispersion of boron on the Al_2O_3 surface, the XPS intensity ratio I(B1s)/I(Al2p) is plotted against the boron loading in Fig. 5. A good linear correlation was obtained and the slope of the line was in good agreement with the theoretical intensity ratio based on Kerkhof-Moulijn monolayer model [24]. These results indicate that boron atoms added by the impregnation are highly and homogeneously dispersed, forming monolayer on the alumina surface up to 2.5 wt% B, in line with the results of Morishige and Akai [8].

Fig. 6 depicts the IR spectra of the OH stretching region of the series of B/Al_2O_3. The spectra of the Al_2O_3 support and MoO_3/B/Al_2O_3 (2.5 wt% B) are also shown. As shown in Fig.6, the IR spectrum of alumina exhibits well-defined OH bands at 3772, 3727, 3677, and 3580 cm^{-1}, in good agreement with those of other workers [25-27]. The 3772, 3727, and 3677 cm^{-1} bands have been assigned to the most basic, basic, and acidic hydroxyl groups respectively, and the band at 3580 cm^{-1} to hydrogen-bonded hydroxyl groups [25,26].

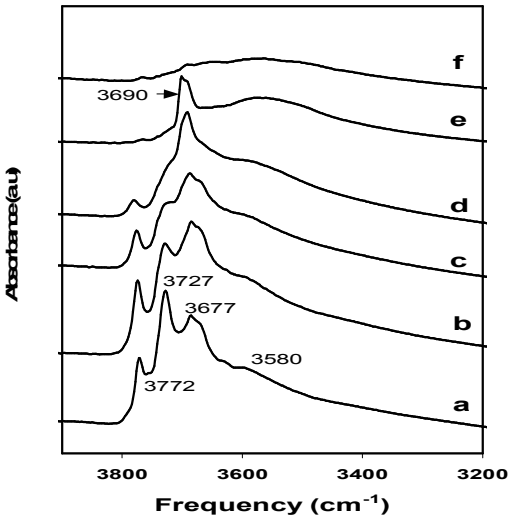

Figure 6 FTIR spectra of OH groups of a) Al_2O_3; b) B/Al_2O_3(0.3 wt% B); c) B/Al_2O_3(0.6 wt% B); d) B/Al_2O_3(1.2 wt% B); e) B/Al_2O_3(2.5 wt% B); and f) $MoO_3/B/Al_2O_3$(2.5 wt% B).

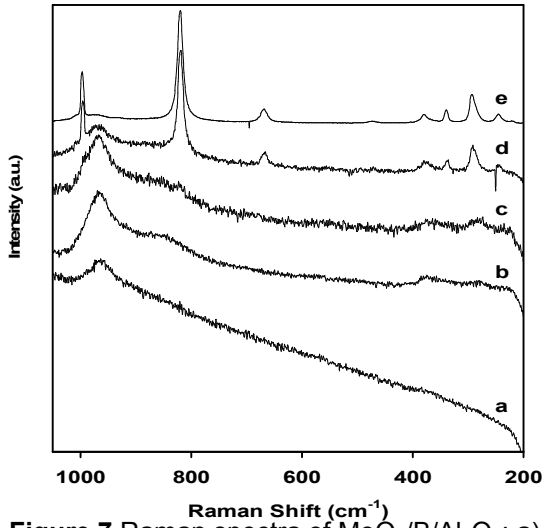

Figure 7 Raman spectra of $MoO_3/B/Al_2O_3$: a) 0 wt% B, b) 0.3 wt% B, c) 0.6 wt% B, d) 0.9 wt% B, and e) 1.2 wt% B.

The addition of 1.2 wt% boron resulted in depletion of the intensity of the IR bands at 3772 cm^{-1} and 3727 cm^{-1}, indicating that boric acid preferentially reacts with the basic alumina hydroxyl groups. The increase of boron loading up to 2.5 wt% B resulted in an almost complete loss of all the OH groups of Al_2O_3 with a new band appearing at 3690 cm^{-1} that corresponds to borate-OH groups, in agreement with the observation of DeCanio and Weissman [25]. In their FTIR analysis of borate-promoted Ni-Mo/Al_2O_3, DeCanio and Weissman [25] reported a complete loss of the OH groups of alumina at 1.5 wt% B. It is clearly shown by the FTIR peak of OH groups of $MoO_3/B/Al_2O_3$ (2.5 wt% B) in Fig. 1 that the OH groups of boron oxides are consumed by the impregnation of Mo oxides. This indicates that Mo oxides are anchored to the OH groups of boron oxides, when the OH groups of alumina are diminished by the addition of boron, leading to weakened interactions between the Mo oxides and the alumina surface.

The Raman spectra of $MoO_3/B/Al_2O_3$ are shown in Fig. 7. Fig. 7 obviously shows that only a band at ca. 960 cm^{-1} appears for the boron-free catalyst, which is assigned to a Mo=O fundamental stretching vibration mode due to small Mo oxide clusters like paramolybdate species [28]. It is likely that the formation of MoO_3 on the boron-free catalyst is entirely excluded by the absence of the sharp peaks due to MoO_3 (Fig. 7). As for the catalysts with boron content up to 0.6 wt% B, the spectra are almost similar to the spectrum of the boron free catalyst, except a very small shoulder peaks at around 990 and 820 cm^{-1}. When the loading of boron reached 0.9 wt% B, a new set of clearly visible bands, which are assigned to crystalline MoO_3, appeared along with a 969 cm^{-1} band. When the loading of boron reached 1.2 wt% B, the peaks due to crystalline MoO_3 predominated at the expense of the highly dispersed Mo oxides characterized by the band around 960-970 cm^{-1}. These results suggest that the addition of boron decreases the dispersion of Mo oxides on the surface of Al_2O_3.

Table 2 Averaged particle size and averaged number of stackings of $MoS_2/B/Al_2O_3$ as observed by TEM

Boron content (wt% B)	Averaged particle size (nm)	Averaged number of stackings
0	4.42	1.40
0.6	4.71	1.66
1.2	5.01	1.82
2.5	5.62	1.71

The averaged stacking number and slab length, as calculated from the TEM images of the $MoS_2/B/Al_2O_3$ are summarized in Table 2. As it is shown in Table 2, the addition of boron promotes the formation of highly stacked MoS_2 particles (≥2 layer) until 1.2 wt% of boron, and this trend levels off at a higher loading of boron. With the size of MoS_2 particles, the boron addition obviously increases the size of MoS_2 particles. The most abundant slab length is in the range of 4-8 nm for the boron-containing catalysts, in contrast to 2-6 nm for the boron-free catalyst. The size of MoS_2 slabs seems continuously increased until the highest loading of boron tested in this research, in conformity with the tendency observed for the NO adsorption (Fig. 2). Larger size of MoS_2 particles will accommodate just a smaller amount of Co to produce the CoMoS phase, in conformity with the

decreasing amount of Co incorporated on the MoS_2 edges of the catalyst by the addition of boron, as presented in Table 2. These results are apparently related to the decrease of the HDS activity at a higher loading of boron (> 0.6 wt%) in Fig. 1.

CONCLUSION

In the present study, we tried to clarify the effect of boron addition on the thiophene HDS activity and the intrinsic activity over $Co/MoS_2/Al_2O_3$. The CVD technique was used to introduce cobalt into the $MoS_2/B/Al_2O_3$ catalyst, in which all the Co atoms form the active sites. The catalysts were characterized by NO adsorption, XPS, Raman spectroscopy, FTIR, and TEM. The salient findings in the present study are as follows:

1. A proper amount of boron addition enhances the HDS activity of CVD-$Co/MoS_2/Al_2O_3$, irrespective of the presulfidation temperature.
2. Boron addition weakens the interaction between Mo oxides and Al_2O_3 surface, hence decreases the dispersion of MoS_2 particles on the Al_2O_3 surface.
3. It is proposed that the addition of boron promotes the formation of pseudo Co-Mo-S type II over CVD-$Co/MoS_2/Al_2O_3$ presulfided at 673 K. The Co-Mo-S pseudo type II is a metastable phase with the TOF value intermediate between Co-Mo-S type I and type II.
4. With CVD-$Co/MoS_2/B/Al_2O_3$ presulfided at 773 K, the addition of boron accelerates the formation of well-crystallized MoS_2 structure to form real Co-Mo-S type II.
5. The CVD technique, in which Co are selectively anchored to the MoS_2 edges of $MoS_2/B/Al_2O_3$, is a promising technique to investigate the nature of additive effects on HDS catalysts on the basis of the number of active sites and their intrinsic activity.

REFFERENCES

1. Song C., 2003, *Catal. Today,* 86, 211
2. Topsøe H., Clausen, B.S., and Massoth, F. E., 1996, Catalysis: Science and Technology, J.R. Anderson, M. Boudard, Eds., Springer-Verlag: Berlin, , Vol.11, p.1
3. Kabe K., Ishihara, A., and Qian, W., 1999, *Hydrodesulfurization and Hydrodenitrogenation*, Kodansha, Tokyo
4. Chianelli R. R., 1984, *Catal. Rev.-Sci. Eng*. 26, 361
5. Prins R., de Beer V. H. J., and Somorjai, G. A., 1989, *Catal. Rev. Sci. Eng.,* 31, 1
6. Song C., and Ma, X. 2003, *Appl. Catal. B,* 41, 207
7. Usman, Kubota, T., Araki, Y., Ishida, K., and Okamoto, Y., 2004, *J. Catal.* 227, 523
8. Morishige H. and Akai. Y., 1995, *Bull. Soc. Chim. Belg.,* 104, 4
9. Li D., Sato, T., Imamura, M., Shimada H., and Nishijima, A., 1998, *Appl. Catal. B,* 16, 255
10. Lewandowski M. and Sarbak, Z., 2000, *Fuel,* 79, 487
11. Ferdous D., Dalai, A. K., and Adjaye, J., 2004, *Appl. Catal. A,* 260, 153
12. Stranick M. A., Houalla, M., and Hercules, D.M., 1987, *J. Catal*., 104, 396
13. Okamoto Y., Ochiai, K., Kawano, M., Kobayashi, K., and Kubota, T., 2002, *Appl. Catal. A,* 226, 115
14. Okamoto Y., Ishihara, S., Kawano, M., Satoh, M., and Kubota, T., 2003, *J. Catal.,* 217, 12
15. Okamoto Y. and Kubota, T., 2003, *Catal. Today* 86, 31
16. Okamoto Y., Ochiai, K., Kawano, M., and Kubota, T., 2004, *J. Catal.,* 222, 143
17. Okamoto Y., Kawano, M., Kawabata, T., Kubota, T., and Hiromitsu, I., 2005, *J. Phys. Chem. B*, 109, 288
18. Ramírez J., Castillo, P., Cedeño, L., Cuevas, R., Castillo, M., Palacios, J. M., and Agudo, A.L., 1995, *Appl. Catal. A,* 132, 317
19. Topsøe N. –Y. and Topsøe, H., 1982, J. Catal., 77, 293
20. Okamoto Y., Kato, A., Usman, Sato, K., Hiromitsu, I., and Kubota, T., unpublished results
21. Breysse M., Portefaix, J. L., and Vrinat, M., 1991, *Catal. Today,* 10, 489
22. Okamoto Y., Imanaka, T., and Teranishi, S., 1981, *J. Phys. Chem.,* 85, 3798
23. Cattaneo R., Weber, T., Shido, T., and Prins, R., 2000, *J. Catal.,* 19, 225
24. Kerkhof F. P. J. M. and Moulijn, J. A., 1979, *J. Catal.,* 83, 1612
25. DeCanio E. C. and Weissman, J. G., 1995, *Coll. and Surf. A,* 105, 123
26. DeCanio E. C., Edwards, J. C., Scalzo, T. R., Storm, D. A., and Bruno, J. W., 1991, *J. Catal.,* 132, 498
27. Okamoto Y. and Imanaka, T., *J. Phys. Chem.,* 1988, 92, 7102
28. Okamoto Y., Ochiai, K., Kawano, M., Kobayashi, K., and Kubota, T., 1988, *Appl. Catal. A,* 226, 115